Transcription Factor NsrR from *Bacillus subtilis* Senses Nitric Oxide with a 4Fe−4S Cluster†

Erik T. Yukl, Mohamed A. Elbaz, Michiko M. Nakano, and Pierre Moënne-Loccoz*

Department of Science and Engineering, School of Medicine, Oregon Health & Science University, 20,000 NW Walker Road, Beaverton, Oregon 97006-8921

Received July 16, 2008; Revised Manuscript Received October 6, 2008

ABSTRACT: In *Bacillus subtilis*, NsrR is required for the upregulation of ResDE-dependent genes in the presence of nitric oxide (NO). NsrR was shown to bind to the promoters of these genes and inhibit their transcription *in vitro*. NO relieves this inhibition by an unknown mechanism. Here, we use spectroscopic techniques (UV−vis, resonance Raman, and EPR) to show that anaerobically isolated NsrR from *B. subtilis* contains a $[4Fe-4S]^{2+}$ cluster, which reacts with NO to form dinitrosyl iron complexes. This method of NO sensing is analogous to that of the FNR protein of *Escherichia coli*. The Fe−S cluster of NsrR is also reactive toward other exogenous ligands such as cyanide, dithiothreitol, and O_2. These results, together with the fact that there are only three cysteine residues in NsrR, suggest that the 4Fe−4S cluster contains a noncysteinyl labile ligand to one of the iron atoms, leading to high reactivity. Size exclusion chromatography and cross-linking experiments show that NsrR adopts a dimeric structure in its $[4Fe-4S]^{2+}$ holo form as well as in the apo form. These findings provide a first stepping stone to investigate the mechanism of NO sensing in NsrR.

The ability to adapt to anaerobic conditions is vital for a great diversity of microorganisms. It is particularly true of pathogenic organisms, which may encounter oxygen limitation within their hosts. Such bacteria also commonly face other stresses such as nitric oxide (NO) produced by phagocytic cells as part of the immune response of the host (*1*). Thus, an understanding of how bacteria sense and respond to these conditions is of considerable importance.

An example of the bacterial response to oxygen limitation is found in *Bacillus subtilis*, which, in the absence of oxygen, can grow by nitrate respiration (*2*). The ResDE two-component regulatory system is required for the induction of genes involved in nitrate respiration (*3*). These genes include *fnr* (the gene encoding anaerobic transcription factor) (*4*), *nasDEF* (nitrite reductase genes) (*5*), and *hmp* (flavohemoglobin gene) (*6*). However, anaerobic conditions alone are not sufficient for the full induction of the ResDE-controlled genes, in particular *hmp* and *nasDEF*, and the presence of NO is required to attain the full induction of these genes (*7*). The effect of NO is abrogated in an *nsrR* mutant strain, indicating a role for NsrR in NO-mediated control of the ResDE regulon (*8*).

NsrR belongs to the Rrf2 family of transcription regulators and is widely found in various bacteria (*9*). Sequence analyses predict that NsrR contains a helix-turn-helix, which likely binds to the promoter region of its target genes (*9*). *In vivo* studies of *nsrR* mutants and the effect of NO on NsrR-controlled genes have shown that NsrR is an NO-responsive transcription repressor in *Escherichia coli* (*10*), *B. subtilis* (*8*), *Salmonella enterica* serovar Typhimurium (*11*), *Neisseria gonorrheae* (*12*), and *Neisseria meningitidis* (*13*). In addition, NsrR was shown to repress ResDE-dependent *in vitro* transcription of *hmp* and *nasD* (*8*). The critical role of NsrR in modulating Hmp levels under both aerobic and anaerobic conditions and its impact on oxidative and nitrosative stress in macrophages was recently exemplified in *S. enterica* serovar Typhimurium (*14*). However, structural information on NsrR remains sparse.

NsrR bears significant homology (30% identity and 48% similarity) to IscR, a 2Fe−2S cluster-containing transcriptional regulator of Fe−S cluster synthesis genes in *E. coli* (*15*). Notably, among the residues conserved between these proteins are three cysteine residues likely to coordinate the iron−sulfur cluster in IscR, although the number of residues separating the first Cys from the CX_5C motif varies in IscR and NsrR orthologues. A transient brownish color in aerobically purified NsrR has suggested that NsrR also contains an Fe−S cluster sensitive to O_2-mediated decomposition (*8*).

Other transcriptional regulators bearing Fe−S clusters whose activities are modulated by NO have been reported. NO binds to the $[2Fe-2S]^{+}$ cluster of SoxR to form a dinitrosyl iron complex (DNIC1) that activates transcription of *soxS* (*16*). Similarly, FNR contains a $[4Fe-4S]^{2+}$ that reacts with NO. However, in this case, NO binding inhibits the transcriptional regulation activity of FNR (*17*). Finally, NO has been shown to react with the 4Fe−4S cluster of aconitase to convert this enzyme into an iron regulatory protein (IRP-1) that controls mRNA translation and stability

† This work was supported in part by Grant GM74785 (to P.M.-L.) from the National Institutes of Health and Grant MCB0818350 (to M.M.N.) from the National Science Foundation. M.A.E. was supported by the International Fellowships Program from the Ford Foundation.

* To whom correspondence should be addressed. Tel: 503-748-1673. Fax: 503-748-1464. E-mail: ploccoz@ebs.ogi.edu.

[1] Abbreviations: DNIC, dinitrosyl iron complex; DTT, dithiothreitol; EPR, electron paramagnetic resonance; IPTG, isopropyl-β-D-thiogalactopyranoside; RR, resonance Raman.

10.1021/bi801342x CCC: $40.75
Published on Web 11/12/2008

by interacting with iron responsive elements (IREs) (*18*−*20*). Thus, there are precedents for the utilization of Fe−S clusters as NO sensors to regulate the activity of Fe−S proteins involved in diverse cellular physiology.

In this article, we use UV−vis, resonance Raman (RR), and electron paramagnetic resonance (EPR) spectroscopies to demonstrate that anaerobically purified NsrR harbors a $[4Fe-4S]^{2+}$ cluster. Size exclusion chromatography and chemical cross-linking experiments are used to determine that NsrR is dimeric in both holo and apo forms. Exposure of this cluster to O_2 leads to its destruction via a $[3Fe\text{-}4S]^{+}$ intermediate. The $[4Fe-4S]^{2+}$ cluster of NsrR also reacts with NO to form at least two distinct forms of DNICs. Other exogenous ligands such as dithiothreitol (DTT) and cyanide (CN^-) are also shown to bind to the Fe−S cluster. We conclude that the 4Fe−4S cluster of NsrR contains at least one labile ligand, either a hydroxide/aqua ligand or a non-Cys endogenous residue, e.g., an aspartate residue as in the 4Fe−4S cluster of *P. furiosis* ferredoxin (*21*−*23*).

MATERIALS AND METHODS

Purification of N-Terminal and C-Terminal His$_6$-Tagged NsrR Proteins (NH-NsrR and CH-NsrR). The various strains and plasmids used in this study are listed in Table S1 (see Supporting Information). The NH-NsrR expression plasmid, pMMN648, was previously constructed (*8*). To produce CH-NsrR, plasmid pMMN740 was constructed as follows. The *nsrR* gene was amplified by PCR from pMMN638 (*8*) using the primers oMN05-296 (5′-GGCGCGGGCATATGAAGT-TAACCAATTATAC-3′) and oMN06-304 (5′-CGCTCTC-GAGTTCCTTCATTTTTAAAAGC-3′). The resulting PCR product was digested with *Nde*I and *Xho*I and cloned into pET-23a(+) (Novagen) digested with the same enzymes. The construct was verified by DNA sequencing analysis. *E. coli* BL21 (DE3)/pLysS carrying pMMN648 or pMMN740 was grown at 37 °C in 1 to 2 L of M9-glucose medium (*24*) supplemented with 40 μM ferric ammonium citrate, 50 μg/mL of ampicillin, and 5 μg/mL of chloramphenicol. At an OD_{600} of 0.4, isopropyl-β-D-thiogalactopyranoside (IPTG) was added to a final concentration of 0.5 mM. After incubating at 37 °C for 3 h, cells were collected by centrifugation at 5,000*g*, resuspended in culture medium, and transferred into a 1-L sealed bottle. The cell suspension was sparged with argon and kept overnight at 4 °C. Cells were broken by passing through a French press placed in a plastic anaerobic glovebag (Glas-Col, LLC) continuously flushed with argon. The cleared lysate was recovered by centrifugation in a sealed tube at 15,000*g* for 20 min. Subsequent purification steps were performed in an anaerobic chamber containing less than 1 ppm O_2 (Omni-Laboratory System; Vacuum Atmospheres Co.). All buffers and solutions were purged with argon and kept in the anaerobic chamber before use.

Cleared lysate was mixed with 15 mL of Ni^{2+}-nitrilotriacetic acid (Ni-NTA) resin (QIAGEN or Sigma) in buffer A (50 mM Tris-HCl, pH 8.5, 100 mM NaCl, 30 mM imidazole). After 1 h of incubation, the column was washed with 10 volumes of buffer A followed by 2 volumes of buffer A containing 1.0 M KCl, 2 volumes of buffer A containing 60 mM imidazole, and 2 volumes of buffer A containing 100 mM imidazole. His$_6$-NsrR was eluted with buffer A containing 300 mM imidazole. Fractions containing His$_6$-NsrR were pooled and exchanged into an imidazole-free buffer containing 50 mM Tris-HCl and 100 mM KCl at pH 8.5 using HiTrap Desalting columns (GE Healthcare). The C-terminal His-tag protein was eluted from the Ni-NTA column in an identical fashion, but 5 mM dithiothreitol (DTT) was added to the exchange buffer to prevent protein precipitation likely due to the poor Fe−S incorporation observed in this construct.

Complementation of nsrR with His$_6$-NsrR. To examine whether CH-NsrR complements the *nsrR* null mutation in *B. subtilis*, two plasmids pMMN749 and pMMN750 were generated. pMMN749 was constructed by cloning the erythromycin-resistance gene isolated from pDG646 (*25*) into pMMN740 digested with *Hin*cII and *Xba*I, and pMMN750 was constructed by cloning the tetracycline-resistance gene from pDG1515 (*25*) into pMMN740 digested with *Hin*cII. pMMN749 and pMMN750 were used to transform a *B. subtilis* strain JH642 (*nsrR*$^+$) to generate ORB7270 and ORB7285, respectively. The transformants were obtained by a single crossover recombination at the *nsrR* locus, resulting in transcription of *ch-nsrR* from the native *nsrR* promoter (Figure S1, Supporting Information). ORB7270 and ORB7285 were transduced with SPβ phage carrying a transcriptional *nasD-lacZ* fusion (*5*) to generate ORB7284 and ORB7287, respectively.

Complementation experiments were carried out by determining the expression of *nasD-lacZ* in ORB7284 and ORB7287 together with LAB2854 (wild type carrying *nasD-lacZ*) (*5*) and ORB6188 (*nsrR* mutant carrying *nasD-lacZ*) (*8*). Cells were grown under anaerobic conditions in 2× YT (*26*) supplemented with 1% glucose and 0.2% KNO_3 or 2× YT supplemented with 0.5% glucose and 0.5% pyruvate with appropriate antibiotics. Cells were collected at 1-h intervals and β-galactosidase activity was measured as previously described (*26*) and was shown in Miller units (*24*).

Western Blot Analysis. LAB2854 (wild type), ORB6188 (*nsrR*), ORB7284, and ORB7287 (both carrying *ch-nsrR*) were grown anaerobically in 2× YT supplemented with 0.5% glucose and 0.5% pyruvate, and cells were harvested at T_0 (the end of exponential growth). The cell lysate was prepared as described previously (*27*), and 15 μg of total protein was applied to a SDS−polyacrylamide (15%) gel. After electrophoresis, the proteins were electroblotted to nitrocellulose membrane filters. The detection of CH-NsrR was carried out using an anti-NsrR antibody raised in rabbit, followed by antirabbit secondary antibody conjugated alkaline phosphatase as described (*8*).

Iron and Protein Determinations. The iron content of NsrR was determined spectrophotometrically with the ferrene assay (*28*). Specifically, 30 μL samples of NsrR at two different concentrations were incubated at room temperature with 3 μL of 38% HCl for 10 min. The samples were centrifuged at 15,000*g* for 15 min to remove denatured protein before the addition of 50 μL of 3 M sodium acetate and 5 μL of 1 M ascorbic acid at pH 5.5. Finally, 5 μL of 3.0 mM 3-(2-pyridyl)-5,6-bis(5sulfo-2furyl)-1,2,4-triazine disodium salt hydrate (ferrene, Aldrich) was added. Absorbance values were measured at 593 nm ($\varepsilon_{593} = 35.5\ mM^{-1}\ cm^{-1}$) and compared to two blanks lacking either NsrR or ferrene. As expected, the same procedure applied to apo-NsrR did not reveal any significant iron. Protein concentrations were

determined by the Bradford assay (*29*) using bovine serum albumin (Sigma-Aldrich) as a standard. However, total amino acid analyses of the holo- and apo-proteins (AAA Service Laboratory Inc., Damascus, Oregon) suggest that the Bradford assay overestimates NsrR concentrations by ~25%. Because NsrR contains no tryptophan, the calculated 280 nm molar extinction coefficient on the basis of the amino acid primary sequence is unreliable. Instead, concentrations of NsrR monomers were calculated using 280 nm molar extinction coefficients deduced from the total amino acid analyses of holo-NsrR ($\varepsilon_{280} = 38$ mM^{-1} cm^{-1}) and apo-NsrR ($\varepsilon_{280} = 24.3$ mM^{-1} cm^{-1}).

Size Exclusion Chromatography. Size exclusion chromatography was performed using a BioSil SEC 250 prepacked size exclusion column (Bio-Rad) with a Varian HPLC system. The protein sample (60 to 100 μM) was loaded and eluted at 1.0 mL/min with argon-purged buffer containing 100 mM potassium phosphate at pH 7.5, 150 mM KCl, and 2.5 mM DTT. Elution profiles were monitored by absorbance at 280 nm. The column was calibrated using a gel filtration standard containing thyroglobulin, γ-globulin, ovalbumin, myoglobin, and vitamin B_{12} (Bio-Rad).

Chemical Cross-Linking. Holo-NsrR was exchanged into the appropriate buffer using HiTrap Desalting columns (GE Healthcare). Apo-NsrR was acquired by extensive aerobic dialysis (~24 h) of holo protein against 50 mM Tris-HCl, 100 mM KCl, 5 mM DTT, and 10 mM EDTA at pH 8.5 at room temperature, followed by dialysis into 50 mM potassium phosphate buffer at pH 7.5, 100 mM KCl, and 5 mM DTT. Holo- and apo-NsrR at 30 to 80 μM were anaerobically incubated with 1.0 mM dimethyl suberimidate dihydrochloride (Fluka) and 100 mM KCl in 50 mM potassium phosphate buffer at pH 7.5. After 1 h of incubation at room temperature, the reaction was quenched with the addition of a 4-fold volume of pure acetic acid (Sigma-Aldrich), and each sample was diluted to ~10 μM protein for analysis by SDS−PAGE (12% gel).

Spectroscopic Characterization of NsrR. All sample preparation steps were performed in the anaerobic chamber. When necessary, samples for spectroscopic analysis were concentrated using filtering devices (Microcon 10 kD cutoff, Biomax, Millipore). Reduced protein was generated by the addition of excess sodium dithionite in the presence or absence of DTT. Oxidized NsrR was generated either by the addition of excess potassium ferricyanide followed by its removal using desalting spin columns (Zeba 0.5 mL; Pierce) or by the addition of DTT to 4.0 mM followed by exposure to O_2 gas. Addition of NO to the headspace of an NsrR sample was performed with a gastight Hamilton syringe to reach a partial pressure of 0.5 atm. After ~5 min of incubation, the samples were exposed to the inert atmosphere of the glovebox to release the excess NO and transferred to EPR tubes (Wilmad Laboratory Glass) sealed with rubber septa. Alternatively, NsrR samples were incubated with varying concentrations of diethylamine NONOate (Sigma-Aldrich) for 1 h at room temperature or diluted 2.5-fold with NO-saturated buffer in a sealed tube and incubated for 5 min. Cyanide complexes were generated by 15-min incubation of reduced NsrR with 20 mM NaCN.

All UV−vis spectra were obtained using a Cary 50 spectrophotometer (Varian). EPR spectra were obtained on a Bruker E500 X-band EPR spectrometer equipped with a superX microwave bridge and a dual-mode cavity with a helium-flow cryostat (ESR900, Oxford Instruments, Inc.) for measurements at 5−10 K and a super HiQ cavity resonator (ESR4122, Bruker) for measurements at 100 K. The experimental conditions, i.e., temperature, microwave power, and modulation amplitude, were varied to optimize the detection of all potential EPR active species and ensure nonsaturating conditions. Quantitation of the EPR signals was performed with Cu^{II}(EDTA) standards.

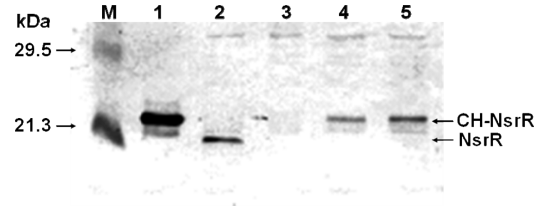

FIGURE 1: Western blot analysis of NsrR. Cleared lysates were prepared from *E. coli* BL21(DE3)/pLysS carrying pMMN740 (lane 1), *B. subtilis* strains LAB2854 (wild type, lane 2), ORB6188 (*nsrR* mutant, lane 3), ORB7284 (*nsrR* mutant carrying pMMN749, lane 4), and ORB7287 (*nsrR* mutant carrying pMMN750, lane 5). Molecular weight markers are shown in the lane marked with M.

Room temperature and low-temperature (110 K) RR spectra were obtained using a 90° and backscattering geometry, respectively. All spectra were collected on a custom McPherson 2061/207 spectrograph (set at 0.67 m with variable gratings) equipped with a Princeton Instruments liquid-N_2-cooled CCD detector (LN-1100PB). Excitation at 488 nm was provided by an Innova I90C-3 argon ion laser, and Rayleigh scattering was attenuated using a long-pass filter (RazorEdge, Semrock). Frequencies were calibrated relative to indene and CCl_4 (room temperature) or aspirin (110 K) and are accurate within ± 1 cm^{-1}.

RESULTS

CH-NsrR Complements an nsrR Mutant in B. subtilis. This study uses both N-terminal and C-terminal His_6-tagged proteins called NH-NsrR and CH-NsrR, respectively. In order to determine whether NH-NsrR is functional in *B. subtilis*, attempts were made to express *nh-nsrR* from the *nsrR* native promoter in a *B. subtilis nsrR* mutant strain, but the N-terminally tagged protein is not produced in *B. subtilis*. Since CH-NsrR and NH-NsrR purified from *E. coli* produce equivalent spectroscopic signatures (see below), we constructed the strains that express *ch-nsrR* from the *nsrR* promoter (see Material and Methods) and determined whether CH-NsrR is expressed in *B. subtilis* at a level similar to that of the native NsrR protein. Strains ORB7284 and ORB7287 do not produce the native NsrR protein and instead produce the tagged NsrR with a molecular weight corresponding to that of CH-NsrR (Figure 1). Furthermore, the level of CH-NsrR produced in the *B. subtilis* strains is similar to that of NsrR in the wild-type strain (LAB2854). These results demonstrate that ORB7284 and ORB7287 are suitable for examining whether CH-NsrR regulates ResDE-controlled genes in the same manner as does native NsrR.

The native NsrR represses *nasD* transcription in anaerobic cultures in the absence of nitrate, while *nasD* expression is derepressed when nitrate is supplied in the medium (Figure 2A). As shown previously (*8*), the effect of nitrate is due to

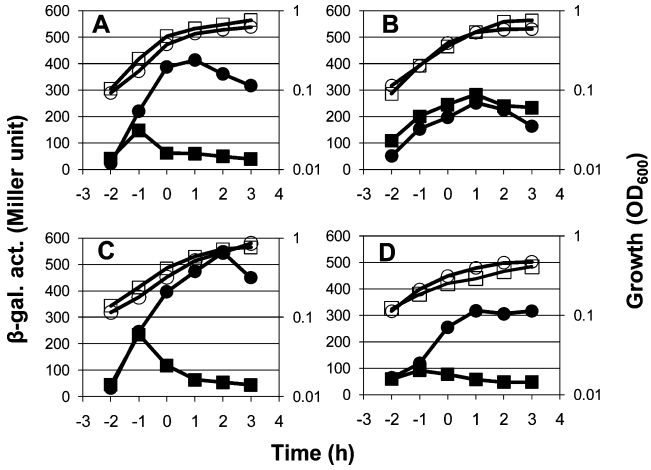

FIGURE 2: Anaerobic expression of *nasD-lacZ* in (A) LAB2854 (wild type), (B) ORB6188 (*nsrR* mutant), (C) ORB7284 (*nsrR* mutant carrying pMMN749), and (D) ORB7287 (*nsrR* mutant carrying pMMN750). *B. subtilis* strains were grown anaerobically in 2xYT supplemented with 1% glucose and 0.2% KNO_3 (circles) or with 0.5% glucose and 0.5% pyruvate (squares); open symbols correspond to growth and solid symbols to β-galactosidase activity. Time zero indicates the end of the exponential growth phase.

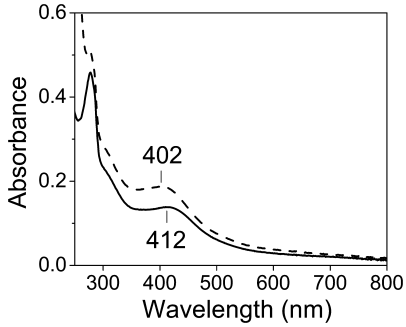

FIGURE 3: Absorption spectra of anaerobically purified NsrR (30 μM) at pH 8.5 in the absence (solid line) and presence (dashed line) of 5 mM DTT.

the NO generated during nitrate respiration. The *nsrR* null mutation alleviates the repression of *nasD* in the absence of nitrate (Figure 2B). In the two strains producing CH-NsrR (Figure 2C and D), *nasD* expression is comparable to that in the wild-type background, indicating that CH-NsrR represses *nasD* transcription, and the repressor activity is sensitive to NO. These results justify the use of CH-NsrR in this spectroscopic study for understanding the Fe−S chemistry that modulates NsrR activity in response to NO.

Holo-NsrR Is a Dimeric Protein Containing a [4Fe−4S]$^{2+}$ Cluster. Anaerobically purified NsrR is greenish brown in color and displays a broad visible absorption feature around 412 nm (Figure 3) characteristic of proteins containing [4Fe−4S]$^{2+}$ clusters (*30*). This assessment is confirmed by the RR and EPR data discussed below. Iron quantitations combined with total amino acid analyses of NH-NsrR yield ~2.8 iron atoms per protein. CH-NsrR showed a substoichiometric iron content per NsrR protein, suggesting much poorer Fe−S cluster incorporation. CH-NsrR also revealed itself as prone to aggregation, presumably due to aberrant disulfide-bond formation between free cysteine residues in protomers lacking the Fe−S cluster. Accordingly, the presence of 5 mM DTT could prevent the aggregation process. Attempts to increase Fe−S cluster occupation by anaerobic

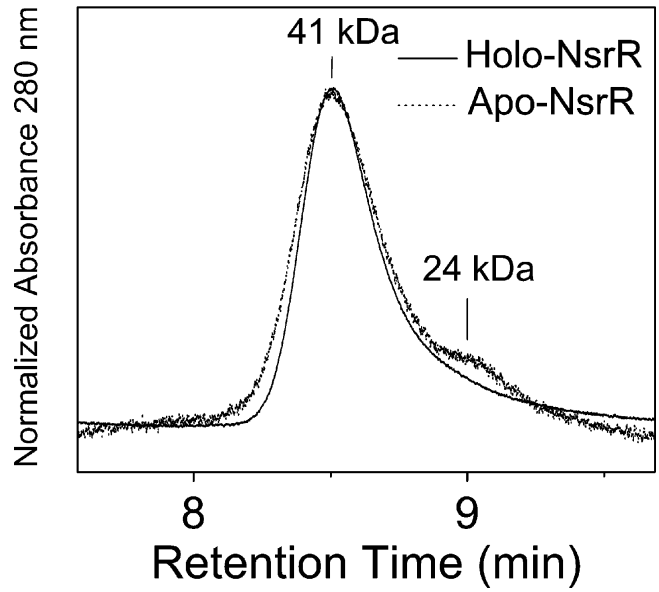

FIGURE 4: Size exclusion chromatography elution profile of anaerobically purified holo-NsrR (65 μM, solid line) and apo-NsrR (92 μM, dashed line) at pH 7.5 monitored at 280 nm.

reconstitution of either CH-NsrR or NH-NsrR using $FeSO_4$ and NaS_2 led to protein precipitation. Despite differences in the extent of Fe−S incorporation in the two constructs, their RR and EPR characterizations, in all redox and coordination states investigated here, were qualitatively identical (Figures S2 and S3, Supporting Information). Thus, further discussions of spectroscopic data and iron/protein ratios are based on data obtained with NH-NsrR.

Assuming that all iron in NH-NsrR is present as 4Fe−4S clusters, the iron quantitation leads to a $\varepsilon_{412} = 14 \pm 1$ mM^{-1} cm^{-1} per 4Fe−4S cluster, which is in good agreement with values observed for other 4Fe−4S proteins (*31*) such as FNR ($\varepsilon_{420} = 13.3$ mM^{-1} cm^{-1}) (*32*). Anaerobic gel filtration of holo-NsrR in the presence of 2.5 mM DTT suggests that, at ~65 μM, holo-NsrR exists exclusively as a dimer with an apparent molecular weight of 41 kDa (Figure 4). This value is in good agreement with the theoretical molecular weight of 39 kDa for the dimer. Apo-NsrR under the same conditions also elutes as a dimer while a small shoulder at 24 kDa is likely to represent a minor monomeric population. The predominance of the dimeric form in both holo- and apo-NsrR is also confirmed by chemical cross-linking experiments. Specifically, holo-NsrR and apo-NsrR incubated with the chemical cross-linker dimethyl suberimidate at two different concentrations were analyzed by denaturing SDS−PAGE and shows the presence of the dimeric form, as indicated by a protein band approximately twice the size of the individual monomers (Figure 5). As expected for this protein concentration range (*33*), no evidence of a significant population of high-order oligomer is observed.

The [4Fe−4S] Cluster of NsrR Contains a Labile Ligand. The room temperature RR spectrum of anaerobically isolated NsrR obtained with a 488-nm excitation exhibits a strong ν(Fe−S) bridging mode at 338 cm^{-1} consistent with a [4Fe−4S]$^{2+}$ cluster and lacks an equally intense band near 290 cm^{-1}, which would support a [2Fe−2S]$^{2+}$ cluster (Figure 6A) (*31*). The RR spectrum is similar to those obtained for oxidized *Clostridium pasteurianum* ferredoxin (*Cp* Fdx) and for reduced *Chromatium vinosum* high potential iron−sulfur

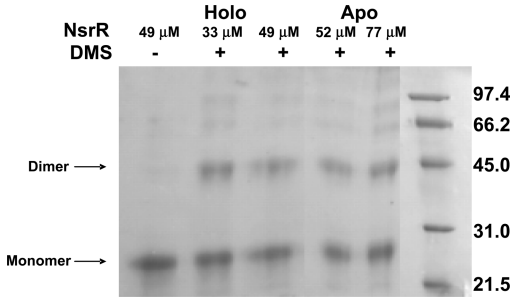

FIGURE 5: Chemical cross-linking of holo and apo-NsrR. The noted protein concentrations were anaerobically incubated in the presence of 1.0 mM dimethyl suberimidate for 1 h before quenching the reaction with acetic acid and subjecting samples to 12% SDS−PAGE analysis.

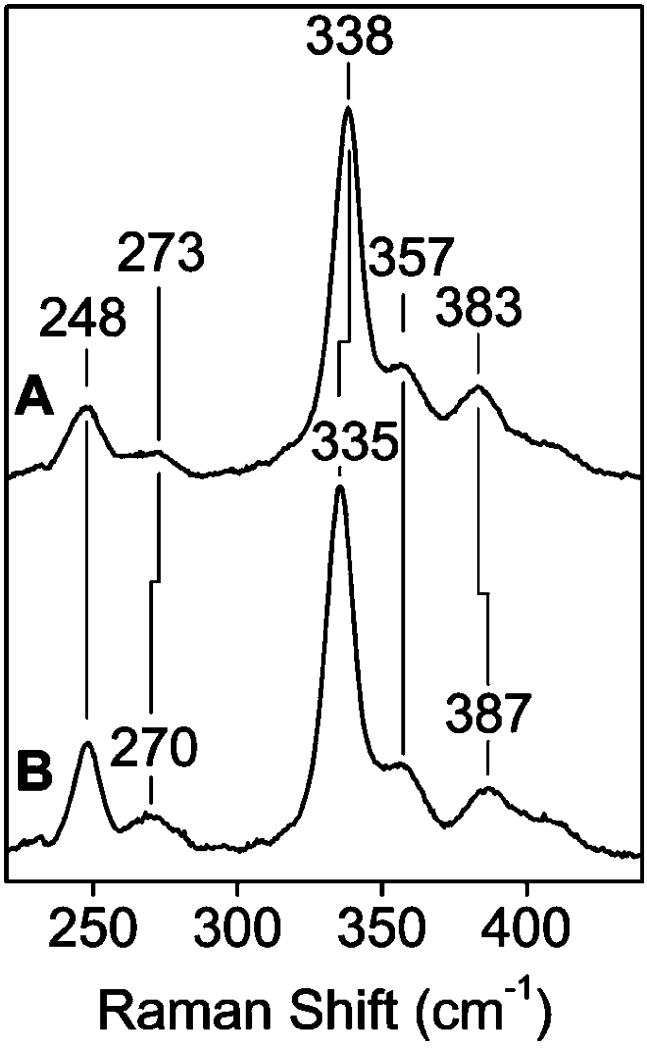

FIGURE 6: Room temperature RR spectra of (A) anaerobically purified NsrR (750 μM) and (B) anaerobically purified NsrR (750 μM) + 5.0 mM DTT (λ_{exc} = 488 nm, 100 mW).

protein at the same excitation wavelength at 77 K (*34*) (see Figure S4, Supporting Information for the low temperature RR spectrum of NsrR). It has been suggested that a high frequency of the totally symmetric ν(Fe−S) bridging mode is characteristic of $[4Fe-4S]^{2+}$ clusters with a non-Cys terminal ligand, as in *Pyrococcus furiosus* ferredoxin where the bridging ν(Fe−S) is found at 442 cm^{-1} in frozen solution (*21*). Although the frequency at room temperature for this mode in NsrR is not unusually high, it is interesting to note a −3 cm^{-1} shift in the presence of DTT (Figure 6B). A

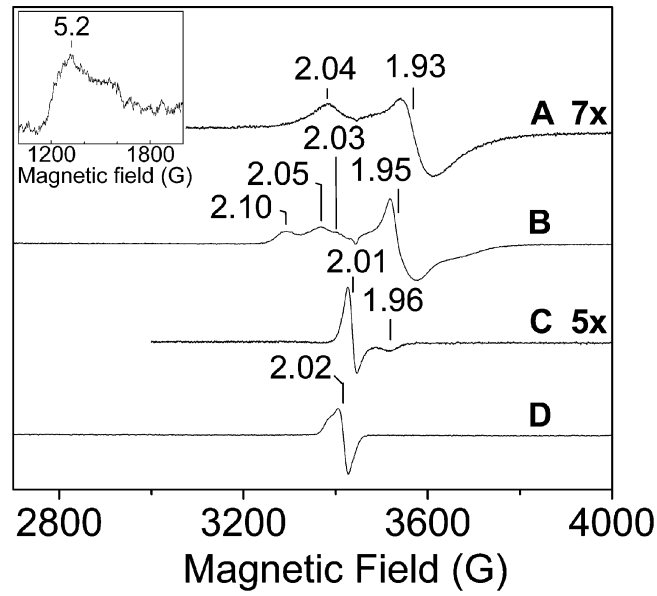

FIGURE 7: EPR spectra of (A) anaerobically isolated NsrR chemically reduced with dithionite (200 μM protein, 0.016 mW microwave power, 10 G modulation amplitude, and T = 10 K), (B) reduced NsrR incubated with 20 mM NaCN (160 μM protein, 0.016 mW microwave power, 10 G modulation amplitude, and T = 10 K), (C) anaerobically isolated NsrR exposed to O_2 in the presence of 4 mM DTT (200 μM protein, 0.005 mW microwave power, and 10 G modulation amplitude), and (D) NsrR in the presence of 1.5 mol equiv of NO from NONOate (160 μM protein, 0.005 mW microwave power, and 10 G modulation amplitude). Inset: EPR spectrum of reduced NsrR highlighting S = 3/2 population (200 μM protein, 10 mW microwave power, 10 G modulation amplitude, and T = 5 K). All spectra have been normalized according to microwave power and sample concentration.

change in the UV−vis spectrum is also observed upon DTT addition (Figure 3). These observations suggest that DTT might bind to one of the Fe ions within the Fe−S cluster.

The as-isolated sample is EPR-silent, as expected for an antiferromagnetically coupled $[4Fe-4S]^{2+}$ cluster (data not shown). Treatment with excess dithionite at pH 8.5 yields a fast-relaxing EPR signal at g = 2.04 and 1.93 observable only below 40 K, as is typical for reduced $[4Fe-4S]^{+}$ clusters (Figure 7A). Attempts at reduction at pH 7.5 were unsuccessful as deduced from a lack of EPR activity in these samples. This is likely due to the increased midpoint potential of dithionite at low pH, particularly when the stock solution may be contaminated with sulfite (*35*), and may be indicative of a fairly low reduction potential of the $[4Fe-4S]^{2+}$ cluster in NsrR.

Quantitation of the reduced NsrR signal against Cu^{II}-EDTA yields 0.18−0.22 spin per 4Fe−4S cluster (as deduced from the UV−vis spectrum of starting material). At microwave powers saturating the S = 1/2 signal, another resonance at g = 5.2 is observed (Figure 7, inset), which likely represents a population of S = 3/2 clusters (*36*) and explains, at least in part, the weak intensity of the S = 1/2 signal. Incubation of reduced NsrR with CN^{-} results in the disappearance of the g = 5.2 signal and produces a new S = 1/2 signal (Figure 7B), which now accounts for 0.64 spin per cluster. These observations are consistent with the coordination of exogenous CN^{-} to convert the $[4Fe-4S]^{+}$ to a pure S = 1/2 species as observed for *Pyrococcus furiosus* ferredoxin (*22*). The remaining spin count missing in the EPR spectra may be due to chelation by the high concentra-

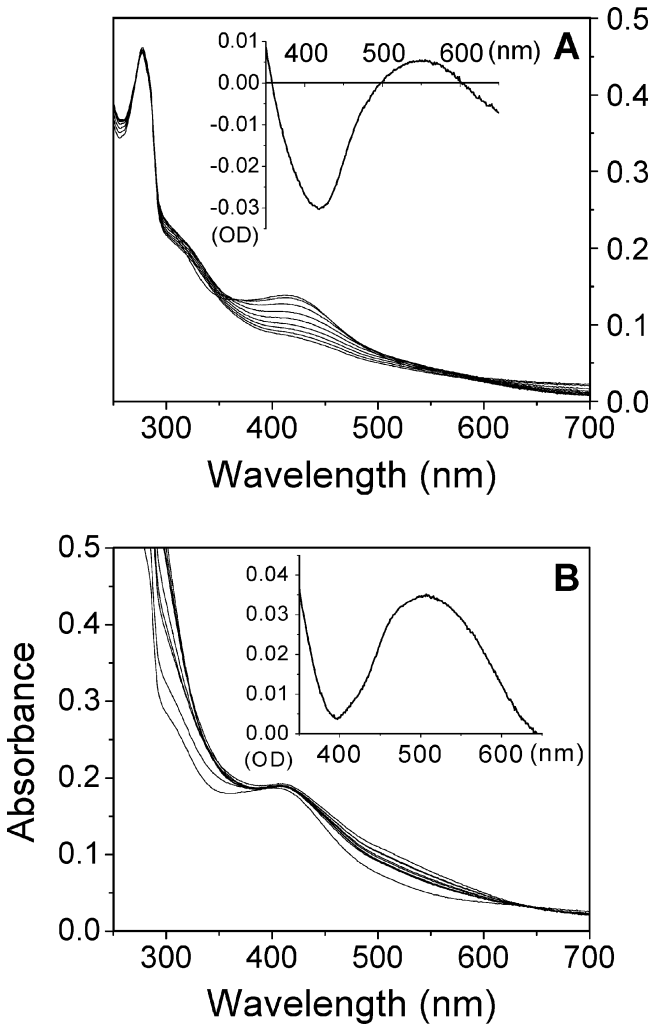

FIGURE 8: UV−vis spectra of (A) NsrR (30 μM) exposed to O_2, with scans taken every 4 min. Inset: Difference spectrum of O_2-exposed NsrR at 14 min minus anaerobic NsrR. (B) NsrR (30 μM) in the presence of 5 mM DTT exposed to O_2, with scans taken every 4 min. Visible absorbance around 500 nm reaches its maximum at 6 min and slowly decays. Inset: Difference spectrum of O_2-exposed NsrR at 6 min minus anaerobic NsrR.

tion of CN^- (20 mM), incomplete reduction of the 4Fe−4S cluster, and/or an overestimation of the cluster concentration caused by adventitious iron in the preparation. In any case, the CN^- binding clearly demonstrates the presence of a labile Fe coordination site in NsrR.

The weak binding of an Fe ligand in NsrR is further illustrated by its reactivity toward O_2. Exposure of anaerobically isolated NsrR to O_2 leads to a bleaching of the $[4Fe-4S]^{2+}$ absorption features (Figure 8A). Difference spectra of the oxygen-exposed samples minus anaerobic NsrR indicate a relative increase in absorbance around 500 nm and a relative decrease at 410 nm, even as the overall absorbance decreases. These changes suggest the formation of a population of $[2Fe-2S]^{2+}$ clusters as previously observed upon exposure of FNR to O_2 (*32*). However, in the case of NsrR, the net decrease in absorbance around 500 nm over time suggests that neither the initial 4Fe−4S cluster nor the 2Fe−2S cluster is aerobically stable.

Interestingly, the presence of 5 mM DTT stabilizes the Fe−S cluster and allows the acquisition of transient UV−vis absorption after exposure to O_2 (Figure 8B). Although

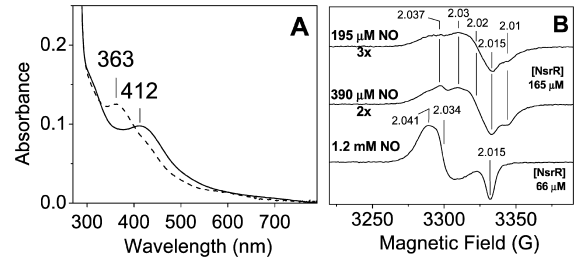

FIGURE 9: (A) Absorption spectra of anaerobically isolated NsrR (24 μM) before (solid line) and after (dashed line) the addition of NO gas. (B) EPR spectra of anaerobically isolated NsrR treated with either saturated NO solution or the indicated concentrations of NO via 1 h incubation with NONOate at pH 7.5 (0.4 mW microwave power, 2 G modulation amplitude, and $T = 100$ K).

absorption features from DTT/Fe(III) complexes may form if iron(III) is released by NsrR and would contribute to these spectra (see Figure S5, Supporting Information), the initial absorption increases observed between 450 and 600 nm are similar to those obtained in the absence of DTT. An EPR analysis of the resulting species yields a narrow spectrum with $g = 2.01$ and 1.96 observable up to 70 K (Figure 7C). This spectrum bears strong resemblance to a $[3Fe\text{-}4S]^+$ cluster as in oxidized *Desulfovibrio fructosovorans* [NiFe] hydrogenase, where the Ni atom is quantitatively lost from the $NiFe_3-S_4$ cluster upon oxidation (*37*). The same species is formed by anaerobic exposure of NsrR to excess ferricyanide (data not shown), but both methods yield only 0.04−0.05 spin per cluster. Again, these data are very similar to those obtained with FNR where only 5−8% of air- or ferricyanide-oxidized samples could be accounted for by the [3Fe-4S] EPR signal (*38*). The remainder may be accounted for by varying populations of EPR-silent $[4Fe-4S]^{2+}$and $[2Fe-2S]^{2+}$ clusters and free iron for samples with longer incubation times. Our UV−vis data show no significant loss of absorbance at 410 nm after 30 min of incubation with O_2 in the presence of 5 mM DTT and suggest that the majority of iron is present as $[4Fe-4S]^{2+}$ and $[2Fe-2S]^{2+}$ clusters.

Anaerobic exposure of NsrR to excess NO gas or dilution in NO-saturated buffer result in the formation of a new chromophoric species with a broad and intense near-UV absorption band at 363 nm (Figure 9A). This optical spectrum is consistent with those of DNICs with extinction coefficients on the order of ~4 mM^{-1} cm^{-1} (*39*), and it suggests that the conversion of the 4Fe-4S cluster into an $[Fe(NO)_2]$ species is efficient. The EPR spectrum of NsrR in a saturated NO solution displays a $g_{av} = 2.03$ (2.041, 2.034, 2.015) axial signal characteristic of $[L_2Fe(NO)_2]^-$ d^7 dinitrosyl-iron(I) complex (DNIC) (Figure 9B) (*40*−*43*). Exposure of NsrR to lower concentrations of NO reveals mixtures of DNIC species with $g_{av} = 2.02$ (Figures 7D and 9B), which are gradually replaced with the more typical 2.033 DNIC signal at high NO concentration (Figure 9B). Quantitations of these EPR spectra range from 0.06 to 0.22 spin per 4Fe−4S cluster for the lowest and saturating NO concentrations, respectively. Thus, only a fraction of the DNIC clusters detected by UV−vis absorption is EPR-active, presumably because of antiferromagnetic coupling between $Fe(NO)_2$ species in DNIC dimers. Similar observations have been reported on DNIC complexes in FNR, another NO sensing transcription factor (*17, 44*). The UV−vis spectra of NO-treated NsrR samples were unaffected by extensive degassing (data not

shown) and suggest that, at least *in vitro*, the DNICs formed in NsrR are irreversible complexes.

DISCUSSION

Fe−S proteins function as versatile regulators by directly sensing O_2, NO, and iron [reviewed in ref *45*]. Previous studies in various bacteria have shown that NsrR is an NO-sensitive repressor, but how NsrR responds to NO remained to be elucidated. The data presented here demonstrate, for the first time, that anaerobically isolated NsrR is a dimeric protein containing a $[4Fe-4S]^{2+}$ cluster. RR characterization of this species yields a spectrum similar to those of other $[4Fe-4S]^{2+}$ clusters in proteins such as certain bacterial ferredoxins and reduced high potential iron proteins (*34*). Reduction of NsrR with excess dithionite yields an EPR-active species with relaxation properties consistent with those of a $[4Fe-4S]^{+}$ cluster. The 4Fe−4S cluster of NsrR shows remarkable reactivity with exogenous ligands such as DTT, CN^-, O_2, and NO. Cyanide binding to native Fe−S clusters has been observed only in *P. furiosus* ferredoxin (*21*) where one of the Fe atoms of the 4Fe−4S cluster is ligated by an Asp residue (*46*). Reports of ligation by exogenous thiols are also scarce, but recruitment of β-mercaptoethanol as a sulfur ligand was observed in Cys/Ala and Cys/Gly mutants of the F_A and F_B clusters in photosystem I (*47*). In the absence of DTT, the labile Fe coordination site in NsrR is likely to be occupied by a non-Cys endogenous residue or an exogenous aqua or hydroxide ligand.

Exposure of NsrR to O_2 results in a gradual degradation of the 4Fe−4S cluster and formation of 3Fe-4S and 2Fe−2S clusters. The addition of DTT stabilizes the $[4Fe-4S]^{2+}$ cluster, although O_2-mediated decay and conversion to $[2Fe-2S]^{2+}$ continue to occur. The reaction of NsrR with NO is also complex and results in the formation of multiple DNIC species. At saturating NO concentration, a typical EPR signal with $g_{av} = 2.03$ reveals the formation of one $(Cys)_2Fe(NO)_2$ per 4Fe−4S cluster. Examination of NO complexes formed at lower NO concentrations reveals more isotropic EPR signals with $g_{av} = 2.02$ that are also suggestive of DNIC species. These multiple EPR signatures for DNIC species in NsrR are in contrast with reports for FNR (*17*), WhiB3 of *Mycobacterium tuberculosis* (*48*), and SoxR of *E. coli* (*16*) where only a single EPR-active DNIC is observed regardless of NO concentration. While the formation of DNICs in NsrR appears irreversible *in vitro*, iron−sulfur repair systems may regenerate the 4Fe−4S cluster of holo-NsrR in *B. subtilis* (*49*−*51*).

The structural picture emerging from this spectroscopic study is that of a 4Fe−4S cluster anchored to a NsrR homodimer via three Cys ligands. Because there are three conserved Cys residues in NsrR, it is tempting to suggest that our construct is limited to half-site cluster loading. However, models where Cys residues from different subunits are recruited for the coordination of the 4Fe−4S cluster cannot be ruled out. Characterizations of Cys variants of NsrR are underway in our laboratories to address this issue.

This *in vitro* characterization of NsrR also provides insight into its function *in vivo*. It has been previously shown that NsrR plays a key role in NO signaling in *B. subtilis* and that aerobically purified NsrR is still capable of repressing *hmp* and *nasD* expression *in vitro* (*8*). It was also shown that the *nsrR* mutation results in derepression of the ResDE-independent expression of *hmp* under aerobic conditions. Thus, apo-NsrR might retain its role as a transcription repressor under aerobic conditions. Possibly, all that is required for DNA binding and gene regulation is for NsrR to adopt a dimeric form, and our size-exclusion chromatography data demonstrate that the presence of Fe−S clusters is not required to stabilize the dimer. In this regard it is interesting that holo-IscR acts as a transcription repressor (*52*), whereas apo-IscR serves as a transcription activator (*53*), and DNA sequences recognized by the two forms of IscR are largely dissimilar. Alternatively, it is possible that within the cell, the 4Fe−4S cluster is stabilized against O_2-mediated decay and that the holo enzyme is responsible for aerobic repression *in vivo*. The *in vitro* stabilization of the 4Fe−4S cluster by DTT suggests that cysteine or other thiol donors may be able to play the same role within the cell; this labile ligand may even provide opportunities for other levels of regulation. Sensing of NO by NsrR occurs via conversion of the Fe−S cluster into a DNIC species. The presence of a labile Fe coordination site in NsrR may provide a simple mechanism to increase the cluster sensitivity to low NO concentrations.

The Fe−S cluster of NsrR shows chemical characteristics similar to those of FNR. Both proteins contain a $[4Fe-4S]^{2+}$ cluster, which upon exposure to O_2 converts to $[2Fe-2S]^{2+}$. However, the $[2Fe-2S]^{2+}$ cluster appears much less stable in NsrR than in FNR. *E. coli* FNR requires the $[4Fe-4S]^{2+}$ cluster to form the transcriptionally active dimer (*54*). In contrast, our gel filtration and cross-linking experiments showed that NsrR is dimeric in both holo and apo forms. Recent work on *B. subtilis* FNR showed that holo- and apo-FNR are dimeric, although a $[4Fe-4S]^{2+}$ cluster is essential for DNA binding and transcription activation (*55*). Unlike *E. coli* FNR where four cysteine residues are essential for its activity (*56*), only three cysteines in *B. subtilis* FNR are indispensable for transcription activation. It was also shown that the three cysteine residues, together with the noncysteine ligand, serve as the ligands for the $[4Fe-4S]^{2+}$ cluster formation. Therefore, *B. subtilis* NsrR shares more chemical features with the iron−sulfur cluster of *B. subtilis* FNR than with that of *E. coli* FNR.

Our current study shows that *B. subtilis* NsrR, like *E. coli* FNR, interacts with NO and forms DNIC (*17*). The DNA-binding activity of FNR is either decreased (*17*) or impaired (*44*) by nitrosylation. It remains to be examined whether NsrR-DNIC exhibits reduced DNA-binding activity, resulting in the loss of repressor activity. Alternatively, nitrosylation of NsrR might change the specificity of DNA binding or affect formation of the transcription initiation complex. Moreover, since different DNIC species are observed depending on the concentration of NO, NsrR may exhibit different responses to different levels of NO concentration. Experiments aimed at testing these hypotheses are underway in our laboratories.

SUPPORTING INFORMATION AVAILABLE

A table listing the strains and plasmids used in this study, a comparison of the RR and EPR spectra of the NH-NsrR and CH-NsrR, and of the room temperature and low temperature RR spectrum of the $[4Fe-4S]^{2+}$ cluster of NH-

NsrR. This material is available free of charge via the Internet at http://pubs.acs.org.

REFERENCES

1. Choi, H. S., Rai, P. R., Chu, H. W., Cool, C., and Chan, E. D. (2002) Analysis of nitric oxide synthase and nitrotyrosine expression in human pulmonary tuberculosis. *Am. J. Respir. Crit. Care Med. 166*, 178–186.
2. Nakano, M. M., and Zuber, P. (1998) Anaerobic growth of a "strict aerobe" (*Bacillus subtilis*). *Annu. Rev. Microbiol. 52*, 165–190.
3. Geng, H., Nakano, S., and Nakano, M. M. (2004) Transcriptional activation by *Bacillus subtilis* ResD: tandem binding to target elements and phosphorylation-dependent and -independent transcriptional activation. *J. Bacteriol. 186*, 2028–2037.
4. Cruz-Ramos, H., Boursier, L., Moszer, I., Kunst, F., Danchin, A., and Glaser, P. (1995) Anaerobic transcription activation in *Bacillus subtilis*: Identification of distinct FNR-dependent and -independent regulatory mechanisms. *EMBO J. 14*, 5984–5994.
5. Nakano, M. M., Hoffmann, T., Zhu, Y., and Jahn, D. (1998) Nitrogen and oxygen regulation of *Bacillus subtilis nasDEF* encoding NADH-dependent nitrite reductase by TnrA and ResDE. *J. Bacteriol. 180*, 5344–5350.
6. LaCelle, M., Kumano, M., Kurita, K., Yamane, K., Zuber, P., and Nakano, M. M. (1996) Oxygen-controlled regulation of the flavohemoglobin gene in *Bacillus subtilis*. *J. Bacteriol. 178*, 3803–3808.
7. Nakano, M. M. (2002) Induction of ResDE-dependent gene expression in *Bacillus subtilis* in response to nitric oxide and nitrosative stress. *J. Bacteriol. 184*, 1783–1787.
8. Nakano, M. M., Geng, H., Nakano, S., and Kobayashi, K. (2006) The nitric oxide-responsive regulator NsrR controls ResDE-dependent gene expression. *J. Bacteriol. 188*, 5878–5887.
9. Rodionov, D. A., Dubchak, I. L., Arkin, A. P., Alm, E. J., and Gelfand, M. S. (2005) Dissimilatory metabolism of nitrogen oxides in bacteria: comparative reconstruction of transcriptional networks. *PLoS Comput. Biol. 1*, e55.
10. Bodenmiller, D. M., and Spiro, S. (2006) The *yjeB* (*nsrR*) gene of *Escherichia coli* encodes a nitric oxide-sensitive transcriptional regulator. *J. Bacteriol. 188*, 874–881.
11. Bang, I. S., Liu, L., Vazquez-Torres, A., Crouch, M. L., Stamler, J. S., and Fang, F. C. (2006) Maintenance of nitric oxide and redox homeostasis by the salmonella flavohemoglobin *hmp*. *J. Biol. Chem. 281*, 28039–28047.
12. Overton, T. W., Whitehead, R., Li, Y., Snyder, L. A., Saunders, N. J., Smith, H., and Cole, J. A. (2006) Coordinated regulation of the *Neisseria gonorrhoeae*-truncated denitrification pathway by the nitric oxide-sensitive repressor, NsrR, and nitrite-insensitive NarQ-NarP. *J. Biol. Chem. 281*, 33115–33126.
13. Rock, J. D., Thomson, M. J., Read, R. C., and Moir, J. W. (2007) Regulation of denitrification genes in *Neisseria meningitidis* by nitric oxide and the repressor NsrR. *J. Bacteriol. 189*, 1138–1144.
14. Gilberthorpe, N. J., Lee, M. E., Stevanin, T. M., Read, R. C., and Poole, R. K. (2007) NsrR: a key regulator circumventing *Salmonella enterica* serovar Typhimurium oxidative and nitrosative stress *in vitro* and in IFN-gamma-stimulated J774.2 macrophages. *Microbiology 153*, 1756–1771.
15. Schwartz, C. J., Giel, J. L., Patschkowski, T., Luther, C., Ruzicka, F. J., Beinert, H., and Kiley, P. J. (2001) IscR, an Fe-S cluster-containing transcription factor, represses expression of *Escherichia coli* genes encoding Fe-S cluster assembly proteins. *Proc. Natl. Acad. Sci. U.S.A. 98*, 14895–14900.
16. Ding, H., and Demple, B. (2000) Direct nitric oxide signal transduction via nitrosylation of iron-sulfur centers in the SoxR transcription activator. *Proc. Natl. Acad. Sci. U.S.A. 97*, 5146–5150.
17. Cruz-Ramos, H., Crack, J., Wu, G., Hughes, M. N., Scott, C., Thomson, A. J., Green, J., and Poole, R. K. (2002) NO sensing by FNR: regulation of the *Escherichia coli* NO-detoxifying flavohaemoglobin, Hmp. *EMBO J. 21*, 3235–3244.
18. Beinert, H., Kennedy, M. C., and Stout, C. D. (1996) Aconitase as iron-sulfur protein, enzyme, and iron-regulatory protein. *Chem. Rev. 96*, 2335–2373.
19. Cairo, G., Ronchi, R., Recalcati, S., Campanella, A., and Minotti, G. (2002) Nitric oxide and peroxynitrite activate the iron regulatory protein-1 of J774A.1 macrophages by direct disassembly of the Fe-S cluster of cytoplasmic aconitase. *Biochemistry 41*, 7435–7442.
20. Rouault, T. A. (2006) The role of iron regulatory proteins in mammalian iron homeostasis and disease. *Nat. Chem. Biol. 2*, 406–414.
21. Conover, R. C., Kowal, A. T., Fu, W. G., Park, J. B., Aono, S., Adams, M. W., and Johnson, M. K. (1990) Spectroscopic characterization of the novel iron-sulfur cluster in *Pyrococcus furiosus* ferredoxin. *J. Biol. Chem. 265*, 8533–8541.
22. Conover, R. C., Park, J. B., Adams, M. W. W., and Johnson, M. K. (1991) Exogenous ligand binding to the $[Fe_4S_4]$ cluster in *Pyrococcus furiosus* ferredoxin. *J. Am. Chem. Soc. 113*, 2799–2800.
23. Hu, Y., Faham, S., Roy, R., Adams, M. W., and Rees, D. C. (1999) Formaldehyde ferredoxin oxidoreductase from *Pyrococcus furiosus*: the 1.85 Å resolution crystal structure and its mechanistic implications. *J. Mol. Biol. 286*, 899–914.
24. Miller, J. H. (1972) *Experiments in Molecular Genetics*, Cold Spring Harbor Laboratory Press, Cold Spring Harbor, NY.
25. Guérout-Fleury, A. M., Shazand, K., Frandsen, N., and Stragier, P. (1995) Antibiotic-resistance cassettes for *Bacillus subtilis*. *Gene 167*, 335–336.
26. Nakano, M. M., Marahiel, M. A., and Zuber, P. (1988) Identification of a genetic locus required for biosynthesis of the lipopeptide antibiotic surfactin in *Bacillus subtilis*. *J. Bacteriol. 170*, 5662–5668.
27. Baruah, A., Lindsey, B., and Nakano, M. M. (2004) Mutational analysis of the signal-sensing domain of ResE histidine kinase from *Bacillus subtilis*. *J. Bacteriol. 186*, 1694–1704.
28. Douglas, J. H., Reid, R. R., Smith, F. E., and Thompson, S. L. (1984) Ferene: a new spectrophotometric reagent for iron. *Can. J. Chem. 62*, 721–724.
29. Bradford, M. M. (1976) A rapid and sensitive method for the quantitation of microgram quantities of protein utilizing the principle of protein-dye binding. *Anal. Biochem. 72*, 248–254.
30. Orme-Johnson, W. H., and Orme-Johnson, N. R. (1982) In *Iron-Sulfur Proteins* (Spiro, T. G., Ed.) pp 67−96, Wiley-Interscience, New York.
31. Duin, E. C., Lafferty, M. E., Crouse, B. R., Allen, R. M., Sanyal, I., Flint, D. H., and Johnson, M. K. (1997) [2Fe−2S] to [4Fe−4S] cluster conversion in *Escherichia coli* biotin synthase. *Biochemistry 36*, 11811–11820.
32. Jordan, P. A., Thomson, A. J., Ralph, E. T., Guest, J. R., and Green, J. (1997) FNR is a direct oxygen sensor having a biphasic response curve. *FEBS Lett. 416*, 349–352.
33. Davies, G. E., and Stark, G. R. (1970) Use of dimethyl suberimidate, a cross-linking reagent, in studying the subunit structure of oligomeric proteins. *Proc. Natl. Acad. Sci. U.S.A. 66*, 651–656.
34. Spiro, T. G., Czeruszewicz, R. S., and Han, S. (1988) in *Biological Applications of Raman Spectroscopy* (Spiro, T. G., Ed.) pp 523−553, Wiley-Interscience, New York.
35. Mayhew, S. G. (1978) The redox potential of dithionite and SO_2^- from equilibrium reactions with flavodoxins, methyl viologen and hydrogen plus hydrogenase. *Eur. J. Biochem. 85*, 535–547.
36. Lindahl, P. A., Day, E. P., Kent, T. A., Orme-Johnson, W. H., and Munck, E. (1985) Mossbauer, EPR, and magnetization studies of the *Azotobacter vinelandii* Fe protein. Evidence for a $[4Fe-4S]^{1+}$ cluster with spin $S = 3/2$. *J. Biol. Chem. 260*, 11160–11173.
37. Rousset, M., Montet, Y., Guigliarelli, B., Forget, N., Asso, M., Bertrand, P., Fontecilla-Camps, J. C., and Hatchikian, E. C. (1998) [3Fe-4S] to [4Fe−4S] cluster conversion in *Desulfovibrio fructosovorans* [NiFe] hydrogenase by site-directed mutagenesis. *Proc. Natl. Acad. Sci. U.S.A. 95*, 11625–11630.
38. Khoroshilova, N., Popescu, C., Munck, E., Beinert, H., and Kiley, P. J. (1997) Iron-sulfur cluster disassembly in the FNR protein of *Escherichia coli* by O_2: [4Fe−4S] to [2Fe−2S] conversion with loss of biological activity. *Proc. Natl. Acad. Sci. U.S.A. 94*, 6087–6092.
39. Costanzo, S., Menage, S., Purrello, R., Bonomo, R. P., and Fontecave, M. (2001) Re-examination of the formation of dinitrosyl-iron complexes during reaction of S-nitrosothiols with Fe(II). *Inorg. Chim. Acta 318*, 1–7.
40. McDonald, C. C., Phillips, W. D., and Mower, H. F. (1965) An electron spin resonance study of some complexes of iron, nitric oxide, and anionic ligands. *J. Am. Chem. Soc. 87*, 3319–3326.
41. Lee, M., Arosio, P., Cozzi, A., and Chasteen, N. D. (1994) Identification of the EPR-active iron-nitrosyl complexes in mammalian ferritins. *Biochemistry 33*, 3679–3687.
42. Vanin, A. F., Serezhenkov, V. A., Mikoyan, V. D., and Genkin, M. V. (1998) The 2.03 signal as an indicator of dinitrosyl-iron complexes with thiol-containing ligands. *Nitric Oxide 2*, 224–234.

43. Foster, H. W., and Cowan, J. A. (1999) Chemistry of nitric oxide with protein-bound iron sulfur centers. Insights on physiological reactivity. *J. Am. Chem. Soc. 121*, 4093–4100.
44. Wu, G., Cruz-Ramos, H., Hill, S., Green, J., Sawers, G., and Poole, R. K. (2000) Regulation of cytochrome *bd* expression in the obligate aerobe *Azotobacter vinelandii* by CydR (Fnr). Sensitivity to oxygen, reactive oxygen species, and nitric oxide. *J. Biol. Chem. 275*, 4679–4686.
45. Kiley, P. J., and Beinert, H. (2003) The role of Fe-S proteins in sensing and regulation in bacteria. *Curr. Opin. Microbiol. 6*, 181–185.
46. Sham, S., Calzolai, L., Wang, P. L., Bren, K., Haarklau, H., Brereton, P. S., Adams, M. W., and La Mar, G. N. (2002) A solution NMR molecular model for the aspartate-ligated, cubane cluster containing ferredoxin from the hyperthermophilic archeaon *Pyrococcus furiosus*. *Biochemistry 41*, 12498–12508.
47. Jung, Y. S., Vassiliev, I. R., Qiao, F., Yang, F., Bryant, D. A., and Golbeck, J. H. (1996) Modified ligands to F_A and F_B in photosystem I. Proposed chemical rescue of a [4Fe−4S] cluster with an external thiolate in alanine, glycine, and serine mutants of PsaC. *J. Biol. Chem. 271*, 31135–31144.
48. Singh, A., Guidry, L., Narasimhulu, K. V., Mai, D., Trombley, J., Redding, K. E., Giles, G. I., Lancaster, J. R., and Steyn, A. J. (2007) *Mycobacterium tuberculosis* WhiB3 responds to O_2 and nitric oxide via its [4Fe−4S] cluster and is essential for nutrient starvation survival. *Proc. Natl. Acad. Sci. U.S.A. 104*, 11562–11567.
49. Overton, T. W., Justino, M. C., Li, Y., Baptista, J. M., Melo, A. M., Cole, J. A., and Saraiva, L. M. (2008) Widespread distribution in pathogenic bacteria of di-iron proteins that repair oxidative and nitrosative damage to iron-sulfur centers. *J. Bacteriol. 190* 2004–2013.
50. Fontecave, M., and Ollagnier-de-Choudens, S. (2008) Iron-sulfur cluster biosynthesis in bacteria: Mechanisms of cluster assembly and transfer. *Arch. Biochem. Biophys. 474*, 226–237.
51. Johnson, D. C., Dean, D. R., Smith, A. D., and Johnson, M. K. (2005) Structure, function, and formation of biological iron-sulfur clusters. *Annu. Rev. Biochem. 74*, 247–281.
52. Giel, J. L., Rodionov, D., Liu, M., Blattner, F. R., and Kiley, P. J. (2006) IscR-dependent gene expression links iron-sulphur cluster assembly to the control of O_2-regulated genes in *Escherichia coli*. *Mol. Microbiol. 60*, 1058–1075.
53. Yeo, W. S., Lee, J. H., Lee, K. C., and Roe, J. H. (2006) IscR acts as an activator in response to oxidative stress for the *suf* operon encoding Fe-S assembly proteins. *Mol. Microbiol. 61*, 206–218.
54. Moore, L. J., Mettert, E. L., and Kiley, P. J. (2006) Regulation of FNR dimerization by subunit charge repulsion. *J. Biol. Chem. 281*, 33268–33275.
55. Reents, H., Gruner, I., Harmening, U., Bottger, L. H., Layer, G., Heathcote, P., Trautwein, A. X., Jahn, D., and Hartig, E. (2006) *Bacillus subtilis* Fnr senses oxygen via a [4Fe−4S] cluster coordinated by three cysteine residues without change in the oligomeric state. *Mol. Microbiol. 60*, 1432–1445.
56. Melville, S. B., and Gunsalus, R. P. (1990) Mutations in FNR that alter anaerobic regulation of electron transport-associated genes in *Escherichia coli*. *J. Biol. Chem. 265*, 18733–18736.

BI801342X